

Modeling Damage to  
Limestone Exposed to  
Atmospheric Pollutants

J.D. Leith, M.M. Reddy,  
J.F. Ramirez

MRS

PROCEEDINGS  
PREPRINT

Printed from Materials Research Society  
Symposium Proceedings Volume 462,  
*Materials Issues in Art and Archaeology V*,  
Sandover, J.R. Druzik, J.F. Merkel, and  
Wright, editors.

## MODELING DAMAGE TO LIMESTONE EXPOSED TO ATMOSPHERIC POLLUTANTS

S.D. LEITH, M.M. REDDY\* and W.F. RAMIREZ

University of Colorado, Department of Chemical Engineering, Box 424, Boulder, CO 80309,  
red.ramirez@colorado.edu

\*U. S. Geological Survey, Water Resources Division, 3215 Marine Street, Boulder, CO 80303,  
nmreddy@gumby.cr.usgs.gov

### ABSTRACT

Preservation of building and monument stone exposed to acidic environments relies on the understanding of acidic precipitation deposition processes and damage mechanisms. Presented here is a model which predicts sulfur accumulation in porous limestone subjected to dry deposition of  $\text{SO}_2$ . The model assumes deposition and reaction of  $\text{SO}_2$  to form a thin gypsum crust on the moist surface of the stone, and subsequent sulfur (as aqueous sulfate) transport and accumulation in the stone interior driven by diurnal wetting and drying of the stone surface. Characterization of the limestone pore structure contributes significantly to the evaluation and interpretation of modeled sulfate transport and accumulation in porous building materials. Predicted sulfur accumulation in the stone interior is dependent on the surface boundary conditions, the stone pore geometry and structure, and the rates and mechanisms of aqueous/solid sulfur partitioning (i.e. adsorption, precipitation and dissolution). Model results are compared to moisture content and sulfur accumulation measured in limestone briquettes exposed to a natural dry deposition environment. The model successfully predicts moisture transport in field-exposed limestone, but overestimates the rate of sulfur accumulation. The model may be improved by quantification of the time dependence of the surface sulfate concentration and better understanding of the sulfate partitioning mechanisms.

### INTRODUCTION

Acidic precipitation continues to be a serious environmental problem in many parts of the world. In addition to severely damaging the ecosystem in affected areas, acidic precipitation takes its toll on widely used building materials such as wood, metal and stone [1-4]. The financial consequences of acidic precipitation are not easy to quantify, but estimates indicate that the direct costs of atmospheric corrosion and corrosion protection in industrial countries is approximately one to three percent of the GNP [5]. Many buildings in the northeastern United States and historically significant art works in Europe are constructed from limestone and are subject to severe damage and/or destruction from acidic attack.

Damage to limestone results from both wet and dry deposition of atmospheric pollutants [1-5]. Dry deposition of sulfur compounds results in an unsightly black gypsum crust on the limestone surface and sulfate accumulation in the stone interior [6]. While stone exposed to dry deposition environments tends to retain surface features (until washed with water), the surface gypsum exfoliation and interior sulfate accumulation can cause irreversible mechanical stresses which lead to crumbling and disintegration of the material. In this regard, dry deposition of sulfur compounds to limestone constitutes a major problem in the preservation of monuments and buildings made with this material.

Successful preservation of limestone exposed to acidic atmospheric environments begins with the recognition of wet and dry deposition mechanisms and a physical understanding of the resulting stone damage process. In this paper we investigate the damage to limestone by dry deposition of atmospheric sulfur compounds and present a modeling approach to predict sulfur accumulation in stone exposed to this type of acidic environment. Many investigators have attempted to describe damage to limestone from dry deposition using empirical, electrochemical and kinetic models, and have had varying degrees of success [7-10]. No investigations to date, however, have examined the role of fluid movement in limestone sulfate accumulation. The approach used in this paper is based on moisture transport, in which wetting and drying of the stone surface (from daily dewfall and evaporation cycles) carries dissolved sulfur species from the stone surface through the pore network by diffusion and convection.

### MODEL DEVELOPMENT

The proposed model of sulfate transport to the interior of the limestone is dependent on both formation of a gypsum layer on the stone surface and the presence of moisture in the stone pores. We assume that the gypsum crust is formed quickly on the limestone surface and then acts as a

sulfate reservoir. Transport of sulfate to the stone interior from the surface reservoir is thought to occur by both diffusive and convective mechanisms and to be driven by repeated cycles of stone surface wetting (by dewfall) and drying (by evaporation) in outdoor exposure. Aqueous sulfate loss along the pore walls is assumed to occur by adsorption, precipitation and / or reaction. The transport and accumulation of sulfate in the limestone interior is modeled as a problem in variably saturated flow through porous media, a complex process influenced by the physical and chemical characteristics of the porous material (limestone), the contaminant (sulfur) and the transport fluid (water). Mathematical description emerges from conservation of mass and definition of the Darcy velocity, the rate of liquid water movement through the porous material [11]. When applied to sulfate transport in limestone, a set of coupled partial differential equations results.

The concentration profile of sulfate in the limestone pores as a function of time and position (i.e. depth into the stone) is described by

$$\phi \frac{\partial cS}{\partial t} = \nabla(\phi SD \nabla c) - \nabla(cv) - r \quad (1)$$

[12] where  $c$  is the concentration of sulfate in the pore water ( $M/L^3$ ),  $\phi$  is the porosity of the limestone ( $L^3/L^3$ ),  $D$  is the diffusion coefficient of sulfate in water ( $L^2/T$ ),  $v$  is the Darcy velocity of the water moving through the limestone ( $L/T$ ) and  $S$  is the pore volume saturation (the ratio of pore volume filled with water to the total pore volume). The transport of sulfate between aqueous and solid phases is described by  $r$ , the net mass transfer rate of sulfate out of the pore water ( $M/TL^3$ ). The Darcy velocity is a function of water permeability through limestone and a pressure driving force,

$$v = -k_H \nabla H \quad (2)$$

where  $k_H$  is the hydraulic conductivity (a measure of permeability expressed in units of  $L/T$ ) and  $H$  is the pressure driving force, called the piezometric head ( $L$ ). Note that hydraulic conductivity and head pressure are functions of the pore volume saturation,  $S$  [11]. Defining the correct mechanism for sulfate exchange between the pore fluid and pore wall, be it adsorption, precipitation or heterogeneous reaction, greatly influences the interpretation and implications of the model results. In the present study, the sulfate deposition process from fluid to pore wall is modeled as Langmuir adsorption in which all sulfate that adsorbs to the carbonate walls is assumed to be precipitated and immobile. Adsorption isotherm data for sulfate on calcium carbonate was measured in the laboratory and used in the model to determine parameters of the isotherm function [12].

Prediction of the sulfate concentration profile requires accounting for the time and spatial distribution of water throughout the pore network. The distribution of water in porous limestone is modeled using the following relationship

$$\phi \frac{\partial S}{\partial t} = -\nabla \cdot (v) \quad (3)$$

where all variables are as previously defined [12]. Numerical solution of the coupled model equations (1) - (3) requires application of appropriate boundary conditions and determination of the functional relationships between fluid pressures ( $H$ ), hydraulic conductivity ( $k_H$ ), and pore volume saturation ( $S$ ). In the present study, the coupled moisture and sulfate transport equations were solved using a finite difference package developed by the U.S. Geological Survey [13-14].

Many researchers have formulated models relating fluid saturation to pressures and permeability [15-17], yet these models can not fully account for the complexity and variability of an actual porous system, such as limestone [18]. For this reason, the relationships between water saturation, pressures and permeability in limestone were determined in the laboratory.

## LIMESTONE CHARACTERIZATION

For this study, a block of limestone was collected from the Salem Formation in the midwestern United States and studied at U.S.G.S. facilities in Denver and Boulder, Colorado. The

stone characterization procedures, composition and mineralogy are discussed elsewhere [12, 19]. The limestone porosity averaged 17.6% using helium gas infiltration and quantitative assessment of the pore structure using nitrogen adsorption and mercury intrusion porosimetry illustrates that the size of the limestone pores falls into two primary size ranges, pores  $> 0.03 \mu\text{m}$  and those smaller than  $0.007 \mu\text{m}$  [19]. The smallest pores contribute greatly to the total pore surface area, which suggests that area-dependent sulfur partitioning mechanisms, such as adsorption and heterogeneous reaction, are likely prevalent in pores of this size [12].

The relationships between the model parameters  $k_H$ ,  $H$  and  $S$  were determined by measurement of water / limestone permeability and hydraulic pressure / saturation behavior in limestone cores [19]. These relationships, needed to solve the model equations, also illustrate the effect of the bi-modal pore size distribution on transport of sulfate. Figure 1 reveals the functional form of the hydraulic conductivity / saturation relationship for wetting and drying of the limestone [19]. The data indicate that the hydraulic conductivity through the limestone is low, even at relatively high water saturations. In fact, the figure illustrates that pore water is immobile at saturations less than 0.60 (i.e.  $k_H = 0$ ). This is explained by the presence of many small pores which spontaneously imbibe and hold water by capillarity. A hydraulic pressure / saturation relationship is illustrated in Figure 2; and these data compliment and are consistent with measurements of hydraulic conductivity. Figure 2 illustrates that hydraulic pressure driven moisture transport (i.e. advection) can only occur at a water saturation greater than 0.60. Below this saturation, moisture transport is independent of changes in hydraulic pressure. Once the stone water saturation falls below 0.60, the pore water is immobile (i.e.  $v = 0$ ) and sulfate transport takes place primarily via diffusive mechanisms through the smallest pores. Conversely, at water saturations greater than 0.60, both advection and diffusion are the principal sulfate transport mechanisms.

## RESULTS AND DISCUSSION

The model was applied to three related problems associated with the transport of water and sulfate in variably saturated limestone, including prediction of moisture transport and sulfate accumulation in field-exposed limestone briquettes. The National Acid Precipitation Assessment Program (NAPAP), a 10-year federally funded study which investigated the sources, transport, and effects of acidic precipitation and related phenomena provided measurements of moisture retention and sulfate accumulation in limestone briquettes exposed to a natural dry deposition environment [1]. Data from one of the NAPAP field sites is used here to evaluate performance of the model.

The model was first applied to the wetting and drying of limestone exposed to constant moisture flux boundary conditions. Simulated saturation behavior during both wetting and drying of limestone was compared to measured limestone saturations under laboratory controlled conditions. Pore volume saturations of limestone blocks as a function of time were determined by measuring the change in weight of three limestone blocks as water was either introduced (by partial immersion) or removed (by evaporation) from the stone surface [12]. The model was then used to simulate the wetting and drying of the limestone blocks. Results from the laboratory measurements and the model predictions are presented in Figure 3. The model performed well in prediction of limestone wetting and drying in the range of stone saturations from 0.55 to 0.80, although the wetting saturations of the stone blocks are slightly underestimated. These results suggest that the model can be used to predict moisture transport in field exposed limestone samples with negligible error by application of appropriate boundary conditions.

The wetting and drying characteristics of limestone exposed in the field were simulated using time periodic moisture flux boundary conditions driven by diurnal variation in meteorological parameters such as air temperature, solar radiation, humidity, and wind speed [12]. All of these parameters were measured continuously at NAPAP field sites and the moisture flux boundary condition was evaluated using these field data. Figure 4 illustrates the relationship between the modeled surface moisture flux boundary condition and the modeled moisture retention characteristics of a representative NAPAP field exposed limestone briquette. A surface moisture flux less than zero represents a period of dewfall (or condensation) and moisture fluxes greater than zero represent an evaporative demand at the stone surface. The limestone moisture content varies in a periodic manner over a limited range of pore volume saturations. This is the effect of the bi-modal pore size distribution, in which the small pores hold large volumes of static water and the largest pores are primarily air-filled. The performance of the model in predicting the wetting and drying behavior of field-exposed limestone was evaluated by comparison to limestone moisture retention characteristics

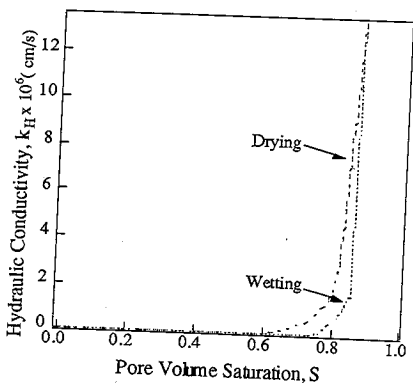


Figure 1. Relationship between hydraulic conductivity and pore saturation as measured in the laboratory. The effect of the bi-modal pore size distribution is to trap water at saturations less than 0.60. In this regime,  $k_H = 0$  and hydraulic pressure driven moisture transport does not occur in the limestone.

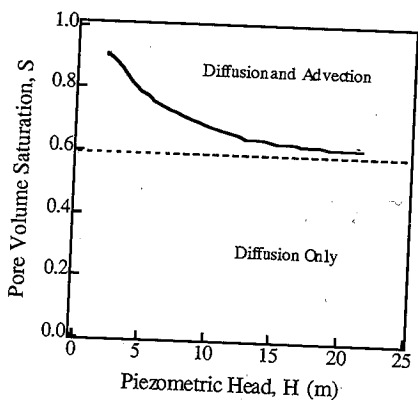


Figure 2. Relationship between applied hydraulic pressure and limestone pore saturation as measured in the laboratory. Diffusive and advective sulfate transport occurs at saturations  $> 0.60$ . Below this saturation, moisture transport is dependent on evaporation and capillarity and sulfate transport occurs by diffusion alone.

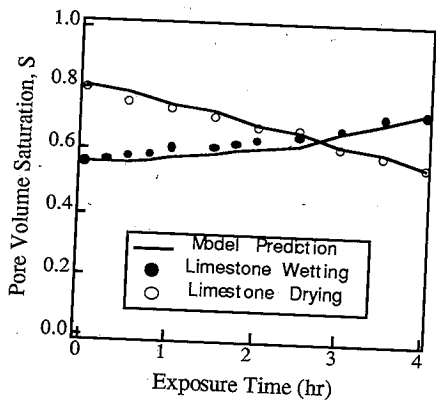


Figure 3. Application of the model to the problem of moisture transport in limestone. Constant surface flux boundary conditions drive the wetting and drying of the stone. The model adequately predicts limestone saturations measured in the laboratory.

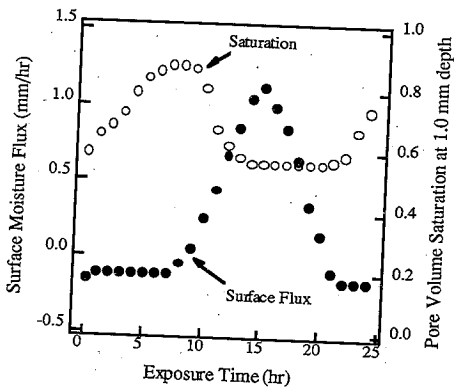


Figure 4. Application of the model to the problem of moisture transport in field-exposed limestone. The diurnal surface moisture flux boundary condition drives the wetting and drying of the stone. The model predicts a periodic saturation history similar to that observed in field-exposed limestone samples.

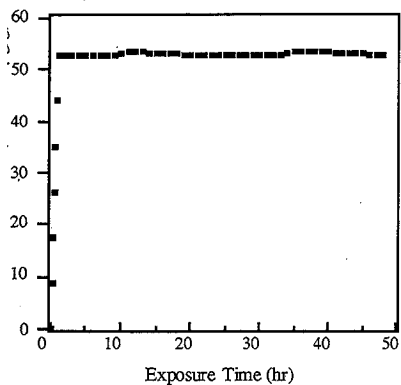


Figure 5. Application of the model to sulfate transport and accumulation in field-exposed limestone. The model predicts rapid sulfate accumulation in the stone interior. Model results presented here represent sulfate accumulation at a stone depth of 250  $\mu\text{m}$ .

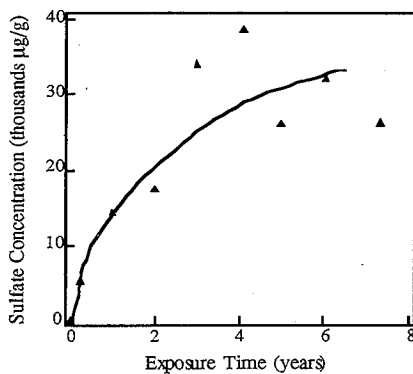


Figure 6. Measured sulfate concentration in first 250  $\mu\text{m}$  of a ground facing, field-exposed limestone briquette. Weathering data collected at Newcomb, NY NAPAP research site from 1984-1991. Actual accumulation of sulfate is much slower than the model prediction (see Figure 5).

ted using a specially designed wetness sensor. In the absence of direct rainfall, both the and the modeled limestone exhibited a diurnal variation in pore volume saturations [12, 20].

The accumulation of sulfate in the ground facing side of field exposed briquettes was modeled using a constant surface concentration boundary condition, that of saturated gypsum solution, and the periodic surface moisture flux boundary condition. Figure 5 illustrates the modeled relationship between exposure time and sulfate accumulation at a depth of 250  $\mu\text{m}$  in a field exposed limestone briquette. Modeled sulfate concentrations were found to rapidly increase to a maximum at a shallow depth of the stone. Simulated exposure time of two days results in a concentration profile representative of the sulfate accumulation at long exposure times in field exposed briquettes. Figure 6 illustrates weathering data collected at a NAPAP field site [12, 21]. Note that the sulfate accumulation is slow and gradual and high concentrations are reached only after years of exposure. Observed weathering behavior is in stark contrast to the model predictions.

The inability of the model to simulate the time dependent weathering behavior of field exposed limestone briquettes is in part due to the use of the constant concentration boundary condition at the stone surface. The surface concentration boundary condition is likely time dependent and is affected by the prevailing surface moisture flux conditions and the concentration of ambient  $\text{SO}_2$ . Recognition of the time dependence of the surface concentration boundary condition would enable the model to predict a time dependent sulfate accumulation profile. Since the model uses the constant boundary condition based on formation of the gypsum crust, our results should be considered as a limiting case. The magnitude of accumulation represents the sulfate concentration at the stone surface after maximum exposure. Oversimplification of the mass transfer partitioning mechanism may lead to error. Using the Langmuir isotherm is a good first approximation to the actual relationship between aqueous and solid sulfur, but this type of mechanism neglects other possible mechanisms for accumulation [12]. Determination of the exact mechanism would necessitate a comprehensive study of sulfur / carbonate chemistry under well controlled conditions.

## CONCLUSIONS

Moisture transport in Salem limestone was predicted by application of fundamental principles describing air and water flow in porous media. Moisture flux boundary conditions were specified based on a surface energy balance and measured meteorological parameters from a NAPAP field site in the northeastern United States. The model predicted limestone saturations in the laboratory with negligible error. Model-predicted wetting and drying behavior of limestone was also compared to moisture retention characteristics of a field-exposed limestone wetness sensor. Both the sensor and the modeled limestone exhibited a diurnal variation in moisture content. The extent of wetting and drying in the limestone briquettes is strongly influenced by the physical nature of the pore structure, specifically, the bi-modal pore size distribution in this material.

The transport and accumulation of sulfate in the variably saturated limestone was modeled using the advection / dispersion equation coupled with equations describing water transport in the stone. The partitioning of aqueous and solid form sulfate was treated using a Langmuir adsorption isotherm based on experimental adsorption measurements. A constant surface concentration boundary condition was specified based on the assumption of a gypsum crust on the stone surface. Results indicate that the present model predicts sulfate concentrations at a limiting condition and not over the entire range of exposure times. The model predicts the sulfate concentration at infinite exposure times. The model may be improved by quantification of the time dependence of the surface sulfate concentration and better understanding of the partitioning mechanism.

## ACKNOWLEDGMENTS

Mike Heymans at Precision Core Analysis assisted in determination and interpretation of limestone permeability measurements. Rick Healy of the U.S. Geological Survey provided valuable assistance in solution of the model equations.

## REFERENCES

1. P.A. Baedecker, E.O. Edney, P.J. Moran, T.C. Simpson, and R.S. Williams in NAPAP report 19, Acidic Deposition : State of Science and Technology. (National Acid Precipitation Assessment Program: Washington, DC, 1990), p. 19-1 - 19-280.
2. M.M. Reddy, *Earth Surf. Proc. and Land.*, 13, p. 335-354, (1988).
3. P.A. Baedecker and M.M. Reddy, *J. Chem. Ed.*, 70, p. 104-108, (1993).
4. Schuster, P.F., M.M. Reddy and S.I. Sherwood, *Mater. Perf.*, 33, p. 76-80, (1994).
5. E. Passaglia in Materials Degradation Caused by Acid Rain, edited by R. Baboian, (ACS Symposium Series 318: Washington, DC, 1986), p. 384-396.
6. E.S. McGee and V.G. Mossotti, *Atmos. Environ.*, 26B, p. 249-253, (1992).
7. T. Skoulikidis, D. Charalambous, and P. Papakonstantinou-Ziotis, *Br. Corros. J.*, 18, p. 200-202, (1983).
8. F.W. Lipfert, *Atmos. Environ.*, 23, p. 415-429, (1989).
9. N.P. Kulshreshtha, A.R. Punuru and K.L. Gauri, *J. Mater. Civ. Eng.*, 1, p. 60-72, (1989).
10. S. Tambe, K.L. Gauri, L. Suhan, and W.G. Cobourn, *Environ. Sci. Technol.*, 25, p. 2071-2075, (1991).
11. J. Bear and A. Verruijt, Modeling Groundwater Flow and Pollution, D. Reidel, Dordrecht, 1987.
12. S.D. Leith, M.S. Thesis, University of Colorado, Boulder, CO, (1993).
13. E.G. Lappala, R.W. Healy and E.P. Weeks, U.S. Geological Survey Water-Resources Investigations Report 83-4099, (1987).
14. R.W. Healy, U.S. Geological Survey Water-Resources Investigations Report 90-4025, (1990).
15. M.T. van Genuchten, *Soil Sci. Amer. Proc.*, 44, p. 892-898, (1980).
16. R. Hambe, K.L. Gauri, and J. Parlange, *Soil Sci.*, 142, p. 325-339, (1983).
17. R.J. Lenhard, and J.C. Parker, *Water Resour. Res.*, 23, p. 2197-2206, (1987).
18. J.C. Parker, *Rev. Geophys.*, 27, p. 311-328, (1989).
19. S.D. Leith, M.M. Reddy, W.F. Ramirez and M.J. Heymans, *Environ. Sci. Technol.*, 30, p. 2202-2210, (1996).
20. R.B. See, M.M. Reddy, and R.G. Martin, *Rev. Sci. Instrum.*, 59, p. 2279-2284, (1988).
21. K.J. Reimann, Argonne National Laboratory Report ANL-89/34, (1991).